Journal of Agricultural Technology 2012 Vol. 8(4): 1413-1421
Available online http://www.ijat-aatsea.com
ISSN 1686-9141

Thresholding of tart-cherry image frame under uncontrolled daylight conditions

M.B. Lak*

Young Researchers Club, Science and Research Branch of Islamic Azad University, Tehran, Iran

M.B. Lak (2012) Thresholding of tart-cherry image frame under uncontrolled daylight conditions. Journal of Agricultural Technology 8(4): 1413-1421.

In order to detect a fruit, a well-defined segmentation algorithm is required. The segmentation process requires finding the adequate thresholds in order to extract the wanted features. In this project 15 methods were applied to determine the thresholds of thirty images in order to detect the tart-cherry fruits. Then, the resulted binary images were assessed. The images were acquired under uncontrolled daylight conditions and the main idea was to find at least one fruit feature in each image. All of the algorithms were based on image gray-levels, i.e. *R* (red), *G* (green), and *B* (blue). Maximum accuracy (90%) was obtained by means of two algorithms which both were based on division of standard deviation of *R* and *G* values on the mean of *i*, meanwhile the minimum accuracy (0%) was based on division of mean of *i* on 255.

Key words: image segmentation, natural luminance, tart-cherry

Introduction

Image segmentation describes the process of dividing an image into non-overlapping, connected image areas (Koschan and Abidi, 2008). The goal of image segmentation is to extract meaningful objects from an input image (Tao *et al.*, 2003) and thresholding is a technique for segmentation of colored or grey scaled images based on the color or grayscale value, which transforms an image into a binary image by transforming each pixel according to whether it is inside or outside a specified range (Huang and Chau, 2008).

Thresholding is a fundamental technique applied in many image processing applications and many relatively simple and computationally effective algorithms have been developed and used for change detection in video sequences (Rosin and Ioannidis, 2003). Tao *et al.* (2003) presented a three-level thresholding method for image segmentation, based on probability partition, fuzzy partition and entropy theory. Bazi *et al.* (2007) presented a novel parametric and global image histogram thresholding method and Huang

*Corresponding author: M.B. Lak; e-mail: mbagher_lak@yahoo.com

and Chau (2008) proposed an approach to search for the global threshold of image using Gaussian mixture model. Xue and Titterington (2010) proposed two median-based approaches.

Application of image processing based methods in agricultural activities has been developed for years. The applications involve activities such as auto-guidance (Benson *et al*., 2003; Han *et al*., 2004), weed control (Nieuwenhuizen *et al*., 2007; Ghazali *et al*., 2009), and post harvest (Naderiboldaji *et al*, 2008; Jahromi *et al.*, 2008). One of the most important applications of image processing is to detect fruits for operations such as, robotic harvesting (Lak, 2010; Bulanon and Kataoka, 2010), ripeness assessment (Junkwon *et al.*, 2009), and yield mapping (Chinchuluun, 2007) which are done under natural daylight conditions and there is no control on the luminance when the images are acquired. Therefore, different thresholds would be required to segment image frames.

The paper suggested coefficient of variation of each gray-scale image as the threshold of that gray-scale image. Then, different methods based on image grayscales means and standard deviations were assessed in order to find thresholds of tart-cherry image frames. The thresholds are required to segment images into binary form. The main idea of this paper was to use variables originated from *RGB* images to estimate the thresholds.

Materials and methods

Thirty digital images were obtained under natural luminance. Image frames were 3072 × 2304 pixels in the *JPEG* format. A digital camera (*Sony, DSC-H5, Color CCD Camera*) was used to acquire the *RGB* images. One of the images is shown in Fig. 1

Fig. 1. Original image in *RGB* color space (rgb-image).

The images were divided into their gray-level images (*R*, *G*, and *B*) and *i* which calculated by Eq.1 (Fig. 2). Descriptive statistics of means and standard deviations of gray-level images are listed in Table 1.

$$i = 3 \times I = 3 \times \frac{r + g + b}{3} = r + g + b \quad (1)$$

Where:
I = image intensity; *r* = first gray-level of original image in *RGB* color space (red); *g* = second gray-level of original image in *RGB* color space (green); *b* = third gray-level of original image in *RGB* color space (blue).

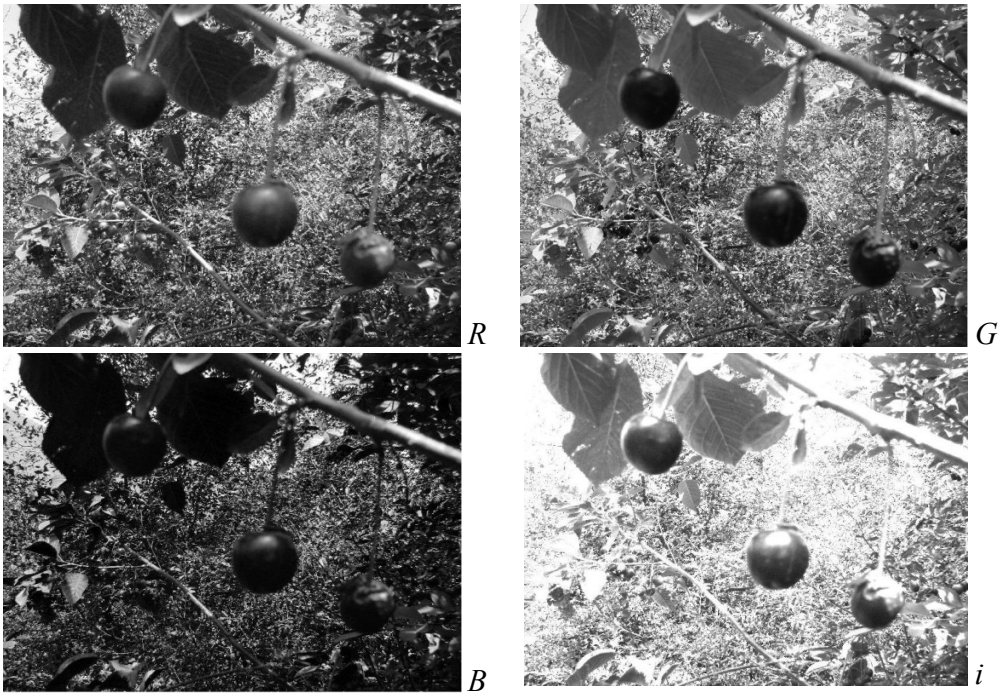

Fig. 2. Gray-level images

Table 1. Descriptive statistics of mean and standard deviation of grayscales

	m^	m_1	m_2	m_3	s	s_1	s_2	s_3
Range	52.3819	36.2146	31.1909	55.1039	33.9571	20.2104	20.4677	50.8736
Min.*	177.2799	79.3828	105.2943	42.8686	44.2985	52.2181	55.1368	50.6740
Max.**	229.6618	115.5974	136.4852	97.9725	78.2556	72.4285	75.6045	101.5476
Mean	195.9576	97.0340	115.6235	68.5777	66.3353	60.9975	63.9018	64.2070
Std.+	14.6147	9.4681	7.9459	14.7914	9.4115	4.7281	5.4410	13.7265
C.V.++	7.4581	9.7575	6.8722	21.5688	14.1877	7.7513	8.5147	21.3785

* Minimum
** Maximum
+ Standard Deviation
++ Coefficient of Variation
^ m, m_1, m_2, m_3, s, s_1, s_2, and s_3 were defined as follow:
m = mean of the i
m_1 = mean of the r
m_2 = mean of the g
m_3 = mean of the b
s = standard deviation of the i
s_1 = *standard deviation of the r*
s_2 = *standard deviation of the g*
s_3 = *standard deviation of the b*

RGB images converted into *YCbCr* color space (Fig. 3) and the third gray-level of ycbcr-image (l) (Fig. 4) was extracted. Then, image t was obtained using Eq. 2 (Fig. 5).

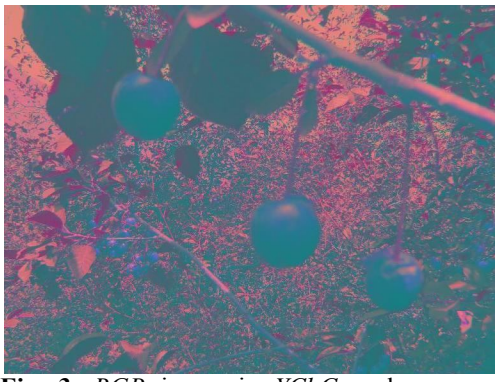

Fig. 3. *RGB* image in *YCbCr* color space (ycbcr-image)

Fig. 4. Third gray-level of ycbcr-image

$$t = 3 \times g - 0.5 \times l \quad (2)$$

Where:
l = third gray-level of the image in *YCbCr* color space

Fig. 5. $t = 3 \times g - 0.5 \times l$

A "*disk*" filter was applied on the t to obtain a noise reduced image (t_2) ($t \xrightarrow{Filtering} t_2$) (Fig.6). The filter diameter was defined as the measure of mean of i in each image frame.

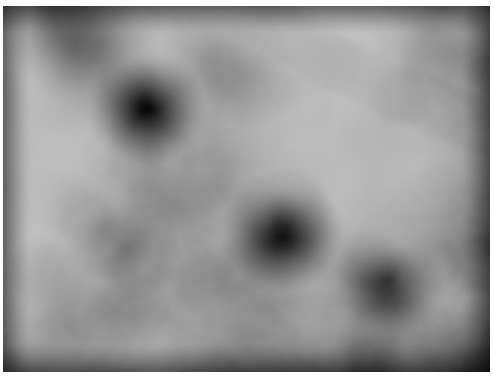

Fig. 6. Image t after filtering (t_2)

Means of 1st, 2nd, and 3rd gray-levels of rgb-image (m_1, m_2, and m_3) were extracted, and the standard deviations (s_1, s_2, and s_3) were calculated. m and s demonstrated the mean and standard deviation of i, respectively.

Filtered images (t_2) then converted into the binary form. 15 thresholding methods were developed in order to obtain binary form of t_2. The methods were all based on m, m_1, m_2, m_3, s, s_1, s_2, and s_3 and their equations are listed in Table 2.

Results and discussions

Fifteen methods were suggested in order to make binary form of the processed images (t_2) (Table 2). Best image segmentation resulted from

thresholds of bw_{10} and bw_{11} (Fig. 7-8), while bw_1 resulted in the worst result (Fig. 9). The accuracy of bw_{10} and bw_{11} where both 90% while bw_1 resulted in the accuracy of 0%.

Table 2. Thresholding methods equations and their descriptive statistics

Method	Equation	Max.	Mean	Min.	Std.	Accuracy (%)
bw_1	$m/255$	0.9006	0.77	0.6952	0.0573	0
bw_2	$m_1/255$	0.4533	0.3803	0.3113	0.0371	83.33
bw_3	$m_2/255$	0.5352	0.4496	0.4129	0.0312	73.33
bw_4	$m_3/255$	0.3842	0.2686	0.1681	0.058	80
bw_5	$s/255$	0.3069	0.2625	0.1737	0.0369	83.33
bw_6	$s_1/255$	0.284	0.2383	0.2048	0.0185	80
bw_7	$s_2/255$	0.2965	0.2494	0.2162	0.0213	80
bw_8	$s_3/255$	0.3982	0.2308	0.1987	0.0538	80
bw_9	s/m	0.4254	0.3691	0.1929	0.0671	76.67
bw_{10}	s_1/m	0.3917	0.3228	0.2358	0.0394	90
bw_{11}	s_2/m	0.4119	0.335	0.2435	0.0419	90
bw_{12}	s_3/m	0.5477	0.3162	0.2296	0.0823	83.33
bw_{13}	s_1/m_1	0.7494	0.6491	0.4947	0.0737	16.67
bw_{14}	s_2/m_2	0.6664	0.5597	0.406	0.0575	30
bw_{15}	s_3/m_3	1.3498	0.9762	0.5645	0.1619	5.56

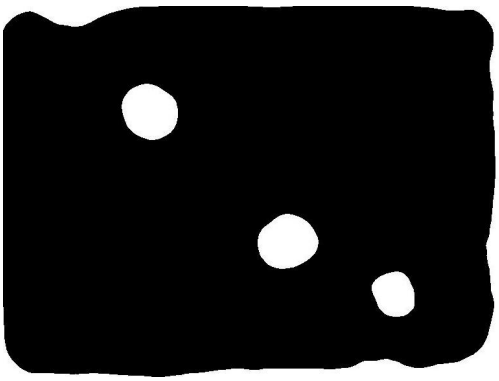

Fig.7. Image bw_{10}

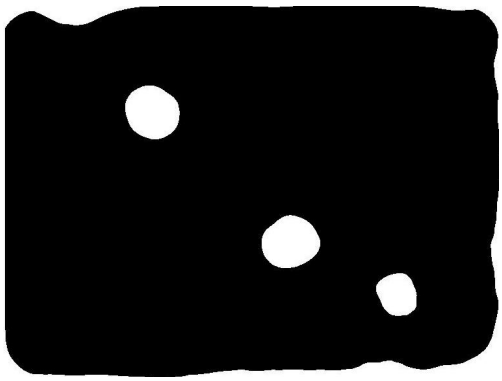

Fig. 8. Image bw_{11}

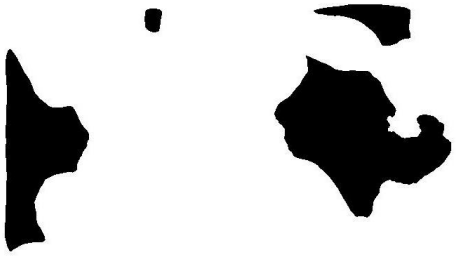

Fig. 9. Image bw_1

Between the methods, bw_{10} and bw_{11} (Table 2) were the best. The methods were based on *R* and *G* standard deviations and the mean of the *i*. Therefore, *R* and *G* gray-levels are more effective than *B* when an image frame of tart-cherry is analyzed. According to Table 1, measures with fewer coefficient of variation resulted in more reliable thresholds. While, fewer coefficients of variations of means and standard deviations of gray-levels may help to find more reliable thresholds.

The worst results (accuracy of 0% and 5.56%) obtained from bw_1 and bw_{15}, respectively. They were based on division of the mean of the *i* on 255 (and the mean of *b* on standard deviation of *b*, respectively.

The error of 10% in bw_{10} and bw_{11} may be due to the uncontrolled luminance conditions. Daylight conditions make shiny and dark regions in the image which lower the algorithm accuracy. Changing color space and filtering reduced the images features and resulted in noise reduced images to obtain better segmentation.

Tao *et al.* (2003) mentioned that their proposed method gave good performance. Xue and Titterington (2010) demonstrated that their two methods (One approach was an extension of Otsu's method, and the other was an extension of Kittler and Illingworth's MET method) could accomplish more robust performance than that of the originals. The main disadvantage of the proposed technique by Bazi *et al.* (2007) is the higher computational time required compared to standard algorithms (which depends on the genetic algorithm used for the identification of the best initial conditions). While the method developed here is low-time consuming, simple, and relatively with high-accuracy.

Conclusion

Thirty images were acquired. The images color space was changed in to *YCbCr*. Then a mathematical equation ($t = 3 \times g - 0.5 \times l$) was developed. t was filtered by a *disk* filter which diameter was m. Fifteen methods were developed and used to thresholding the images when they were converted into binary form. Two methods were better than the others. They were based on R and G standard deviations and mean of i. Their accuracy was both 90%. It is suggested to more focus placed on developing methods based on R and G gray-level images. Fewer coefficients of variations of means and standard deviations of gray-levels also help find more reliable thresholds. For further development, it is suggested to develop three-level thresholding based on maximum fuzzy entropy and genetic algorithm but the required time for the purposed methods must be reduced.

References

Bazi, Y., Bruzzone, L. and Melgani, F. (2007). Image thresholding based on the EM algorithm and the generalized Gaussian distribution. Pattern Recognition 40:619-634.

Benson, E.R.; Reid J.F.; Zhang, Q. (2003). Machine vision-based guidance system for gricultural grain harvester using cut-edge detection. Biosystems Engineering 86(4): 389–398.

Bulanon, D.M. and Kataoka, T. (2010). Fruit detection system and an end effector for robotic harvesting of Fuji apples. Agric Eng Int: CIGR Journal. 12(1): 203-210.

Chinchuluun, R. (2007). Machine vision based citrus yield mapping system on a continuous canopy shake and catch harvester. 78p. Thesis (M.E.) - University of Florida, Florida.

Ghazali, K.H., Mustafa, M.M. and Hussain, A. (2009). Machine vision system for automatic weeding strategy in oil palm plantation using image filtering technique. International Journal of Electrical, Computer, and Systems Engineering 3(4):193-197.

Han, S., Zhang, Q., Ni, B. and Reid, J.F. (2004). A guidance directrix approach to vision-based vehicle guidance systems. Computers and Electronics in Agriculture 43: p.179–195.

Huang, Z.K. and Chau, K.W. (2008). A new image thresholding method based on Gaussian mixture model. Applied Mathematics and Computation 205(2): 899-907.

Jahromi, M.K., Mohtasebi, S.S., Jafari, A., Mirasheh, R., Rafiee, S. (2008). Determination of some physical properties of date fruit (cv. Mazafati). Journal of Agricultural Technology 4(2): 1-9.

Junkwon. P., Takigawa, T., Okamoto, H., Hasegawa, H., Koike, M., Sakai, K., Siruntawineti, J., Chaeychomsri, W., Sanevas, N., Tittinuchanon, P. and Bahalayodhin, B. (2009). Potential application of color and hyperspectral images for estimation of weight and ripness of oil palm (Elaeis guineensis Jacq. Var. tenera). Agricultural Information Research 18(2): 72-81.

Koschan, A. Abidi, M. (2008). Digital color image processing. John Wiley and Sons, Inc., New Jersey. 375 p.

Lak, M.B. (2010). Evaluation of appropriate conditions of image segmentation for tree fruit recognition for mechanized harvesting of apple. 102p. Thesis (M.Sc.) - Science and Research Branch of Islamic Azad University, Tehran, Iran.

Naderiboldaji, M., Jannatizadeh, A., Tabatabaeefar, A. and Fatahi, R. (2008). Development of 11 Mass Models for Iranian Apricot fruits based on some physical attributes (cv. Shahroud-8 and Gheysi-2). Journal of Agricultural Technology 4(1): 65-76.

Nieuwenhuizen, A.T., Tang, L., Hofstee, J.W., Muller, J., Henten, E.J.V. (2007). Colour based detection of volunteer potatoes as weeds in sugar beet fields using machine vision. Precision Agriculture 8: 267–278.

Rosin, P.L., Ioannidis, E. (2003). Evaluation of global image thresholding for change detection. Pattern Recognition Letters 24:2345-2356.

Tao, W.B., Tian, J.W. and Liu, J. (2003). Image segmentation by three-level thresholding based on maximum fuzzy entropy and genetic algorithm. Pattern Recognition Letters 24: 3069-3078.

Xue, J.H. and Titterington, D.M. (2011). Median-based image thresholding. Image and Vision Computing 29(9): 631-637.

(Published in July 2012)